Development and Validation of Control Moment Gyroscopic Stabilization

Undergraduate Honors Research Thesis

By

Gregory R. Colvin

Presented in Partial Fulfillment of the Requirements for Graduation with Research Distinction in Mechanical Engineering from The Ohio State University

Advisors:

Prof. Giorgio Rizzoni & Prof. Ümit Özgüner

Department of Mechanical and Aerospace Engineering

The Ohio State University

February 2014

Abstract

Two wheeled vehicles offer many advantages over other configurations such as greater maneuverability, smaller size, and greater efficiency. These advantages come at the sacrifice of stability and safety. The goal of this work is to improve the stability and safety of a two wheeled vehicle by the development of Control Moment Gyroscopic Stabilization. This technology integrated into a vehicle can deliver unparalleled maneuverability and stability for users compared to any vehicle in use today. The goal of my work was to develop and validate the system of gyroscopic stabilization to be implemented into a vehicle. To validate the concept, a MATLAB/Simulink program was created, modeling the behavior and response of an unstable body with gyroscopic stabilization applied. After completing multiple simulations on this model, a physical structure, similar to an inverted pendulum, was constructed and CMG stabilization has been tested on this setup. Gyroscopic stabilization has been validated in this configuration and has led to further study in multiple degree of freedom situations. The implementation of a vehicle which utilizes this technology can generate safer and more maneuverable vehicles for the public, military, and recreational users.

Acknowledgments

I would like to acknowledge my advisor Prof. Ümit Özgüner and the other members of the Ohio State Agile Rugged Terrain Vehicle team: Prof. Keith Redmill, Michael Vernier, and Simon Kalouche. I would also like to acknowledge C.G. Cantimere Ph.D. for his design work, without which this project would not have been possible. Finally, I would like to acknowledge Daniel Kestner of the OSU department of Physics for his assistance in the derivations of the governing equations which have proven invaluable to my research.

Table of Contents

List of Tables

List of Figures

Chapter 1: Introduction

The Ohio State University Agile Rugged Terrain Vehicle (OSU ARTV) team, funded by the Air Force Research Laboratory, is working towards the development of an off-road vehicle which utilizes Control Moment Gyroscopic (CMG) technology to provide unprecedented maneuverability and agility. Due to the nature of the project, no details of the vehicle are included in this thesis, and it will strictly discuss the development and validation of CMG technology.

Theoretically, there are several ways to stabilize a two-wheeled vehicle; however, only two methods have been demonstrated to date. The most common method of stabilization is dynamic stabilization, i.g. steering or shifting weight. The second method is Control Moment Gyroscopic (CMG) stabilization, which is the subject of this research. This method has the advantage of being more easily controlled by onboard systems than active steering systems and will not interfere with the driver's input steering angle. Also, this system is highly effective at zero speed which is impossible to achieve using active steering and difficult to achieve by shifting mass. Finally, using CMG stabilization the driver would not need to be trained for operating a two-wheeled vehicle as in the case of a motorcycle or bicycle.

Although not very intuitive, CMG stabilization has been demonstrated since the beginning of the 20th century, but success was very limited due to the high cost of motors and bearings at the time. Two of the most famous vehicles that utilized this technology are the Schilovsky Gyro car (Figure 1) and Brennan`s Monorail (Figure 2). Both of these vehicles were successful in operation but due to the price it proved more practical to

Figure 2: Schilovsky Gyro Car

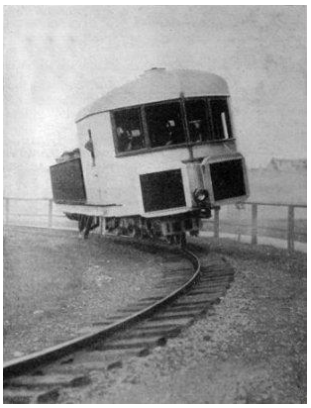

Figure 1: Brennan`s Monorail

continue with four-wheeled vehicles and bi-rail systems. To date, significant progress has been made in both motors and bearings, and electronics allow for onboard systems to control the stabilization instead of a human operator.

Within the modernization and implementation of this technology my research was to develop a model of our system and implement that into MATLAB/Simulink. Once this was completed, I began to develop rudimentary control for the system that varies the CMG behavior and system input values. This work validated the CMG technology and the simulations were then given to other members of the team to further develop using active control techniques. The final portion of my research was the development of a physical test setup to further validate CMG stabilization and give the team an opportunity to test their control systems before implementation onto a vehicle.

This thesis contains four chapters. Chapter 2 discusses the derivation of CMG technology, Chapter 3 contains the validation of CMG technology, and Chapter 4 summarizes the results, presents the key contributions of this thesis, and proposes future directions of study.

Chapter 2: Derivation of CMG Stabilization

2.1 Background

The gyroscope has a long history of application in engineering design due to two properties: rigidity and precession. Rigidity is an important characteristic of gyroscopes where a spinning gyroscope will maintain its orientation in space. This property is utilized in many sensor applications such as navigation systems and passive stabilization systems used in torpedoes or ships. The gyroscope can also be used as an actuator by utilizing the precession phenomenon.

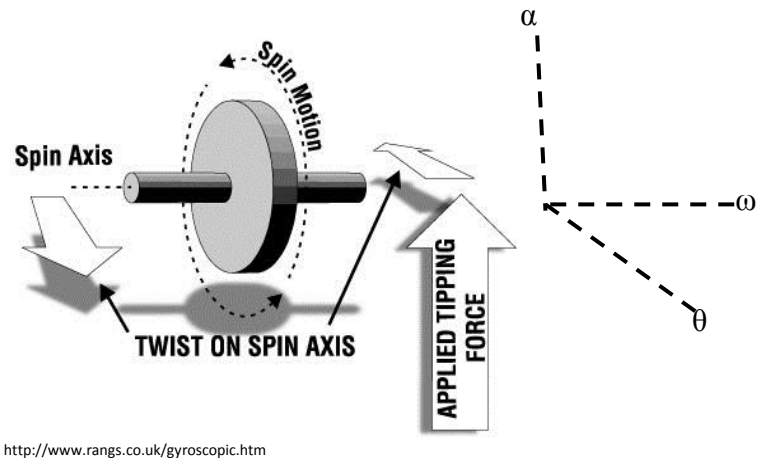

Figure 3: Gyroscopic Precession

CMG systems use conservation of angular momentum to stabilize unstable bodies by functioning as an actuator using the phenomenon of gyroscopic precession. When a flywheel is spinning about the ω axis, if a external disturbance is applied about the θ axis (i.e. a bump in the road) if it has sufficient angular momentum it will stay horizontal and begin to spin around the α axis. This spin about the α axis is called precession and is illustrated in Figure 3.

To utilize this phenomenon for stabilization the flywheel precession axis is attached to the frame such that the precession torque is transferred to the vehicle. In systems which contain CMG stabilization when there is an instability about the θ axis the spinning flywheel is twisted, or gimbaled, about the α axis. This results in a torque about the θ axis which can move the system back into a stable position. Throughout this thesis the rotation of the flywheel will be about the ω axis, the flywheel will be gimbaled about the α axis and the system will be experiencing instabilities about the θ axis.

2.2 Model and Derivation

To begin development, our system was modeled as an inverted pendulum with one degree of freedom about the θ axis and a gyroscope on top, shown in Figure 4. The gyroscope, contains a flywheel, housing, motor, and a gimbaling mechanism. The speed of the flywheel was kept constant, therefore there are two degrees of freedom θ and α, yielding two coupled 2nd order ordinary differential equations to solve. To derive these equations, a brute force Lagrangian approach was used. The variables used nit his derivations can be found in Table 1 below.

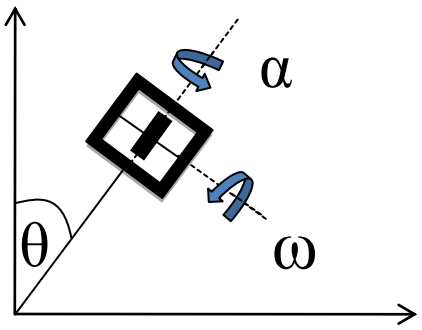

Figure 4: System Model

Table 1: Table of Variables

α	Gimbal angle
θ	Angle from stable position
ω	Rate of rotation (constant)
I_b	Moment of inertia of the body
M_f	Mass of the flywheel
M_g	Mass of the gyroscope
g	Acceleration of gravity
h_{cg}	Height of the center of gravity
r_f	Radius of the flywheel
R	Distance to the center of flywheel

$$\mathcal{L}(\theta, \alpha) = T - V \qquad (1)$$

The kinetic energy equals the energy of the failing body plus the energy in the gyroscope:

$$T = \frac{1}{2} I_b \dot{\theta}^2 + \frac{1}{2} \int dM_f \left(\dot{\vec{x}}\right)^2 \qquad (2)$$

The potential energy is due to gravitational potential, therefore:

$$V_0 = M_b g h_{cg} + M_g g R \qquad (3)$$

$$V = V_0 \cos\theta \quad (4)$$

The difficulty in solving this system is explicitly computing the kinetic energy of the gyroscope, $\frac{1}{2} \int dM_f \left(\dot{\vec{x}}\right)^2$,as a function of θ and α. Completing this equation yields an explicit function $\mathcal{L}(\theta, \alpha)$ which will give the equations of motion. The solution was completed with the assistance of Daniel Kestner, a PhD. candidate of the Ohio State University department of Physics. The full derivation is included in Appendix A.

The solution of this lagrangian is:

$$\mathcal{L}(\theta, \alpha) =$$

$$\frac{1}{2}(I_b + M_g R^2 + \frac{1}{4} M_f r_f^2 (1 + (\sin\alpha)^2))\dot{\theta}^2 + \frac{1}{8} M_f r_f^2 \dot{\alpha}^2 -$$

$$\frac{1}{2} M_f r_f^2 \omega\theta \sin\alpha + \frac{1}{4} M_f \dot{r_f^2} \omega^2 - V_0 \cos\theta \qquad (5)$$

From the lagrangian:

$$\frac{d\mathcal{L}}{d\theta} = \frac{d}{dt}\left(\frac{d\mathcal{L}}{d\dot{\theta}}\right) \quad (6)$$

Solving this yields the first of two O.D.E. `s which describes the system:

$$0 = \left(I_b + M_g R^2 + \frac{1}{4} M_f r_f^2 (1 + (\sin\alpha)^2)\right)\ddot{\theta} + \frac{1}{2} M_f r_f^2 \sin\alpha \cos\alpha\, \dot{\alpha}\dot{\theta} - V_0 \sin\theta - \frac{1}{2} M_f r_f \omega \frac{d}{dt}(\sin\alpha) \qquad (7)$$

Similarly:

$$\frac{d\mathcal{L}}{d\alpha} = \frac{d}{dt}\left(\frac{d\mathcal{L}}{d\dot{\alpha}}\right) \quad (8)$$

Solving this yields the second equation needed to describe the system:

$$0 = \ddot{\alpha} - \sin\alpha \cos\alpha\, \dot{\theta}^2 + 2\omega\dot{\theta}\cos\alpha \qquad (9)$$

These results were found to hold true with previous research [1], and were confirmed by the use of a motion analysis MatLab.

These two highly coupled 2nd order ODEs , equations 7 & 9, would be very difficult to work with if they could not be simplified. Looking at the highest order term in both equations it can be seen that the first equation is used to describe the motion of the body about the θ axis and the second equation describes the motion of the gyro about the α axis. This second equation describes the motion of the gyro if it were allowed to freely rotate about the α axis as the body moved about the θ axis. Here is where an important control can be made: the gyro gimbaling will be actuated by a servo motor, so if we assume that the motor can overcome any natural precession torque and actuate the

gyro, then $\ddot{\alpha}$ becomes an input rather than an output and the system simplifies to the first equation.

Chapter 3: Validation of CMG Stabilization

3.1 MATLAB/Simulink Model

Following the derivation of the underlying equations, a Simulink model was created to simulate the system under a variety of conditions. Equation 7 was rewritten in the form:

$$\ddot{\theta} = \frac{V_0 \sin\theta + B\omega\cos\alpha - B\sin\alpha\cos\alpha\dot{\alpha}\dot{\theta}}{A + \frac{B}{2}(\sin\alpha)^2} \qquad (10)$$

Where:

$$A = I_b + M_g R^2 + \frac{1}{4} M_f r_f^2 \qquad (11)$$

$$B = \frac{1}{2} M_f r_f^2 \qquad (12)$$

Equation 10 was then programmed into Simulink and MATLAB shown in the block diagram and code on the next page. The purpose of this code was not to generate active control for the pendulum but to observe the behavior of the system under different conditions. To use this simulation the user must input material properties of the inverted pendulum and gyroscope so that A, B, and V_0 can be calculated. Then the user inputs an initial instability angle θ which the CMG system will try to correct. Finally the user can manipulate the gimbaling rate $\dot{\alpha}$ to see how the body will react to different gimbaling behavior.

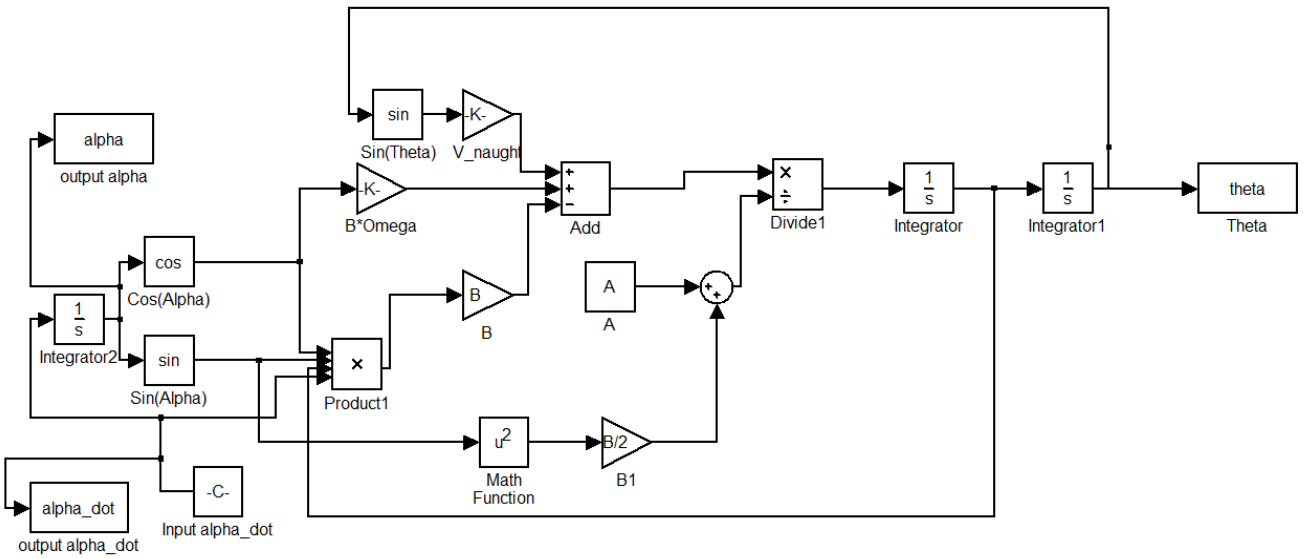

Figure 5: Simulink Block Diagram

```
%input to this code is alpha_dot(gimbal speed)
%output is alpha(gimbal position) and theta
clc;
clear;
%input material properties
Iarm = .89; %moment of the arm(kg/m^2), not including gimbal
Mg = 5.9; %mass of gyro (kg)
Mf = 2.9; %mass of flywheel (kg)
Ma = 3.87; %mass of arm (kg)
R = .083; %distance to center of flywheel (m)
r = .0605; %raduis of flywheel (m)
Hcg = .22 %height of arm center of gravity (m), not including gimbal
w = 10000*pi()/(180*60); %flywheel speed (rad/s) input in rpm then converted
%calculate constants for simulink
A = Iarm+Mg*R^2+(1/4)*Mf*r^2;
B = (1/2)*Mf*r^2;
V_naught = (Ma*Hcg+Mg*R)*9.8;
%%user inputs
alpha_dot =[0:-10:-100];              %% set alpha in rad/sec
theta_i = 5*pi()/180;                   %%set intial theta
%%run simulink code
sim('tabletopsim.mdl');
%%Plot Results
subplot(3,1,1)
plot(t,theta*180/pi())
xlim([0,3])
ylim([0,90])
xlabel('Time(s)');
ylabel('Theta(Degrees)')
subplot(3,1,2)
plot(t,alpha*180/pi())
xlim([0,3])
ylim([0,360])
xlabel('Time(s)');
ylabel('alpha(Degrees)')
subplot(3,1,3)
plot(t,alpha_dot*180/pi())
xlim([0,5])
xlabel('Time(s)');
ylabel('alpha dot(Degrees/s)')
```

Figure 6: MATLAB Code

The output of this code is the pendulum position θ, and also shows the input gimbal rate $\dot{\alpha}$ and gimbal position α. The goal was to vary the gimbal behavior as to bring the pendulum back to a stable position from the initial angle. To achieve this goal the pendulum position θ and all of its derivatives need to be zero at some positive time. This was tested by varying the gimbal rate and observing the resulting pendulum behavior. A secondary goal was to have the gimbal position, α, reach zero at the same time as θ reaches zero so that the system is prepared to handle the next instability. An example of this is shown in Figure 7.

From the simulations in Figure 7, and similar simulations, two main properties were observed. First, and most importantly, it was shown that stabilization of the pendulum could be achieved. To demonstrate this, the plots in Figure 7 will be used as an example. The plot of θ shows the position of the pendulum about the θ axis as a function of time. An initial angle of 10 degrees was selected for the system to overcome. The second, or $\dot{\alpha}$, plot shows the user input gimbal behavior used to try and overcome the initial instability. The plot in Figure 7 contains five different simulations. Each simulation begins with an initial constant gimbal rate and then changes to an exponential decaying rate at a pre-determined time. With this gimbal behavior it can be seen that initially the pendulum falls toward 90 degrees, but then, changes directions at various times and moves back towards a stable position of zero degrees. Some of the initial gimbal rates were too slow resulting in the pendulum falling to 90 degrees. Similarly, some of the gimbal rates are too fast resulting in the pendulum passing 0 degrees and falling to -90 degrees. The middle line of the plots shows a successful trial. For the middle simulation θ and its derivatives reach approximately zero at .325 seconds,

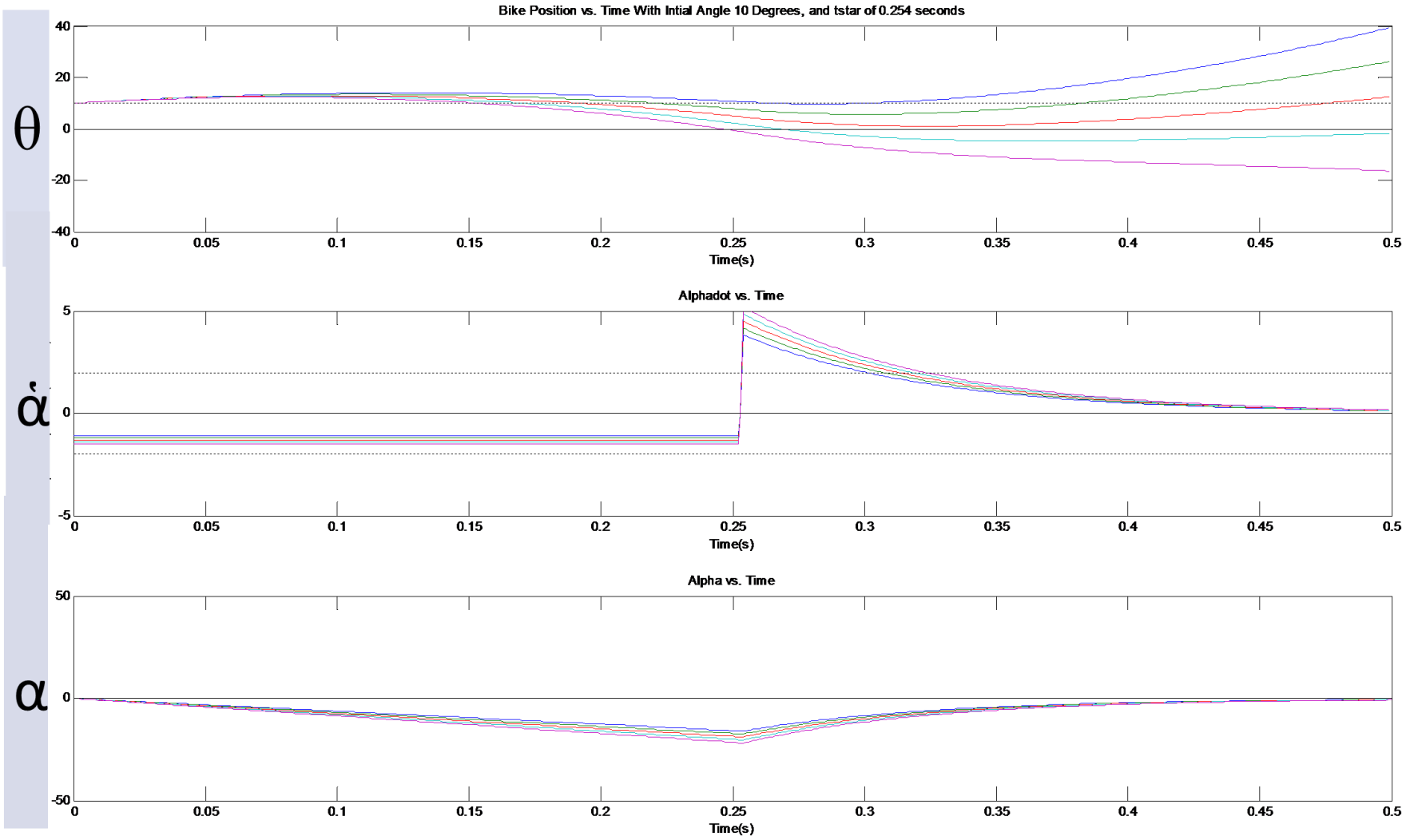

Figure 7: Simulation Results

if the gimbaling were to be stopped at this time the pendulum would be in a stable position, completing the first goal, and the gimbal position α is close to zero, almost completing the second goal.

The second property observed from these simulations was that as the gimbal position leaves zero and approaches 45 degrees the effective corrective torque decreases. This is because as the gyro gimbals the spin axis, ω, also twists. As the ω axis changes orientation only a portion of the axis stays in alignment with the original ω axis, and the rest becomes in alignment with the θ axis. This split in orientation causes the reactive torque to also be split about the θ axis as well as the originalω axis. A torque about the original ω axis does nothing to correct the pendulum position. At the α equal to 45 degree position the reactive torque is split equally about the θ and originalω axis, any more gimbaling causes the majority of the reactive torque to to be about the original ω axis. It can be concluded that it is best to minimize the amount of gimbaling to upright the pendulum and that the gyro should never pass α equal to 45 degree position.

Upon the completion of this and similar simulations the control portion of the project was passed on to Michael Vernier a PhD. student in the ECE department at the Ohio State University. Following this transition my work shifted to experimental validation of CMG stabilization.

3.2: Experimental Validation

To continue the validation of CMG stabilization, a test-setup similar to the modeled inverted pendulum, was designed as seen in Figure 8. This setup is referred to as the Table Top. The flywheel spins at 10,000 RPM about the ω axis powered by a motor (not shown). The flywheel is inside a housing, which is mounted to a vertical shaft, that goes through two bearings, and attaches to a servo motor (orange). This servo gimbals the gyro about the α axis, to generate corrective torque.

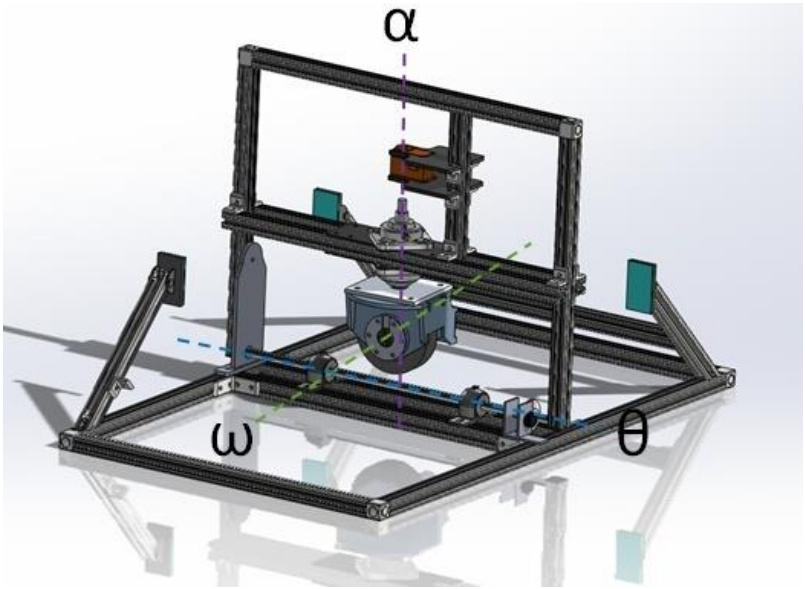

Figure 8: Table Top CAD

This gimbaling system is mounted on an arm, constructed of T-slotted aluminum bars, which rests on an axle inside of two bearings. These bearings allow the arm to rotate freely about the θ axis. The bearings are mounted on a base, also constructed of T-slotted aluminum bars. Mounted on the arm axle is a gear which meshes with another gear mounted on the base. These gears are connected to a quadrature optical encoder that gives feedback on the position of the arm about the θ axis. Finally, attached to the base are four catchers with foam cushion to stop the arm from falling completely over in the case of a malfunction.

Control hardware was designed by Michael Vernier and is described in Figure 9 on the next page. A BeagleBone embedded system is used to maintain the flywheel speed

and servo gimbal rate. Sliding mode control was developed to control the gimbaling and maintain the arm in a vertical position. The fully outfitted Table Top is pictured below in Figure 10.

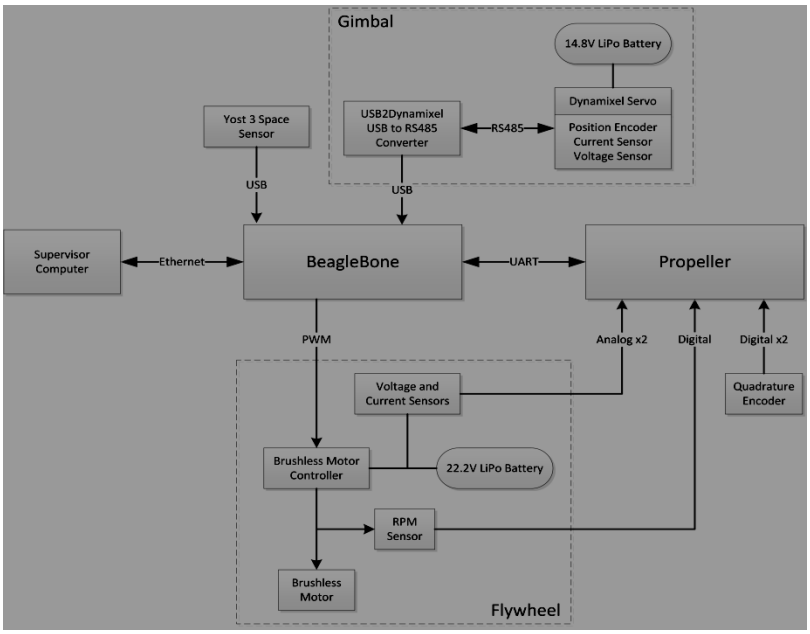

Figure 9: Control Hardware Block Diagram

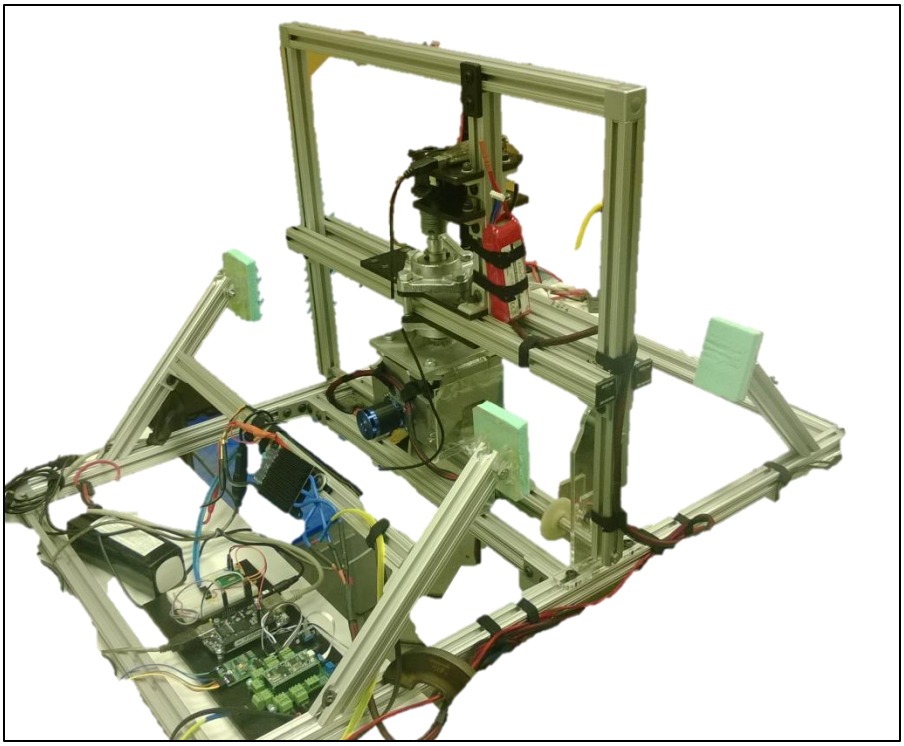

Figure 10: Outfitted Table Top

The large arm used in the Table Top offers many advantages over traditional inverted pendulums. There are inherent risks with a rapidly spinning flywheel and this design is quite robust, reducing risk if there were any malfunctions. In addition the flywheel can be raised and lowered allowing for the team to test given different centers of gravity of the arm. Finally, resting the arm on an axle allows for the use of an optical encoder. This is advantageous because its signal is easier to process than other types of position sensors, allowing easier control. The team took advantage of this by first controlling the pendulum using the encoder and then testing different sensors on the setup with the encoder giving redundancy to the system. This is important because a vehicle will not be able to use an encoder and must use some other type of sensor.

Chapter 4: Results and Conclusions

4.1: Results

Using a sliding mode controller developed by Michael Vernier and Harun Yetkin the Table Top was successfully able to stay upright by gimbaling the flywheel. With refinement of the control code, the system became robust enough to handle large disturbances such as a large push by the user. When pushed the gyro gimbals to bring the arm back to a vertical ($\theta=0$) position and then bring the gyro back to its original centered position ($\alpha=0$). This allows the table top to recover from rapid disturbances. This success has validated control moment gyroscopic stabilization, and the team will continue the development of a prototype vehicle.

4.2 Conclusions and Future Work

The team has continued work on CMG stabilization by developing a second test setup by attaching a gimbaling flywheel to a bicycle. This allows for testing with more degrees of freedom than the Table Top while closely mimicking the prototype vehicle. This test setup has had similar success to the Table Top, and is able to stay vertical and recover from large disturbances from the user. For more information on the bicycle setup please see references 5 &6. The team will continue by implementing this technology into a prototype vehicle and if successful, eventually develop a full size vehicle which uses CMG stabilization to offer unparalleled maneuverability and stability compared to any vehicle in use today.

References

[1] Gallaspy, Jason Matthew. *Gyroscopic stabilization of an unmanned bicycle*, M.S. thesis, Electrical Engineering Department, Auburn University, AL

[2] Meriam, J.L. and Kraige L.G.. *Engineering Mechanics: Dynamics*. 2nd Edition. New York: John Wiley & Sons, Inc., 1986.

[3] Richardson, K.I.T.. *The Gyroscope Applied.* New York: The Philosophical Library, 1955.

[4] Scarborough, James B.. *The Gyroscope: Theory and Applications*. New York: John Wiley & Sons, Inc., 1958

[5] Yetkin H., Kalouche S., Vernier M., Colvin G., Redmill K., Ozguner U.. *Gyroscopic Stabilization of an Unmanned Bicycle, American Control Conference*, Portland, Oregon, 2014

[6]Yetkin, Harun. *Stabilzing Control of an Autonomous Bicycle*. Electronic Thesis or Dissertation. Ohio State University, 2013.

Appendix A: Derivation of Governing ODE's for The Motion of a Gyro on a Hinge

There are 2 degrees of freedom, θ and α. Treating the gyro as a thin plate, we will derive two coupled 2nd order O.D.E's for θ and α. We will use a brute force langrangian approach.

$$L(\theta, \alpha) = \mathrm{T} - \mathrm{V}$$

Where:

$$\mathrm{T} = kinetic = \frac{1}{2} I_{bike} \dot{\theta}^2 + \frac{1}{2} \int_{GYRO} dm \left(\dot{\vec{x}}_{GYRO}\right)^2$$

$$\mathrm{V} = \text{gravitational potential} = \left((\mathrm{M_{BIKE}})(g)\left(h_{BIKE_{CG}}\right) + M_{GYRO} * R \right) \cos\theta = \mathrm{V_o}$$

Euler-Lagrange Equations:

$$\frac{\partial \mathrm{L}}{\partial \theta} = \frac{d}{dt}\left(\frac{\partial \mathrm{L}}{\partial \dot{\theta}}\right)$$

$$\frac{\partial \mathrm{L}}{\partial \alpha} = \frac{d}{dt}\left(\frac{\partial \mathrm{L}}{\partial \dot{\alpha}}\right)$$

These will give us our two ODE's.

The only hang up is that we need to explicitly compute the kinetic energy of the gyro, $\frac{1}{2}\int dm\left(\dot{\vec{x}}_{GYRO}\right)^2$, as a function of α and θ. Once we do that, we will have an explicit function (the Lagrangian), L(θ,α) from which we can get the equations of motion.

To initiate this integral define a coordinate system $\hat{e}_1, \hat{e}_2, \hat{e}_3$, that is fixed to the gyro and which rotates along with it. Every chunk of the gyro is nicely coordinated in this basis. Note that in general $\hat{e}_1, \hat{e}_2, \hat{e}_3$ will point in random directions with respect to $\hat{x}, \hat{y}, \hat{z}$.

$$\vec{x}_{GYRO} = \vec{R} + u\cos\phi\ \hat{e}_1 + u\sin\phi\ \hat{e}_2$$

Note that u and ϕ are time independent coordinates that permit $\int dm\left(\dot{\vec{x}}_{GYRO}\right)^2$ to be written as $\int_0^{r_G}\int_0^{2\pi} \mu * u\ du\ d\theta\ \left(\dot{\vec{x}}_{GYRO}\right)^2$ where μ is the (surface) mass density of the gyro and r_G is its radius.

$$\left(\dot{\vec{x}}_{GYRO}\right)^2 = (\dot{\vec{R}} + u\cos\phi\ \dot{\hat{e}}_1 + u\sin\phi\ \dot{\hat{e}}_2)^2$$

$$= \left(\dot{\vec{R}}\right)^2 + (u\cos\phi\ \dot{\hat{e}}_1 + u\sin\phi\ \dot{\hat{e}}_2)^2 + 2\dot{\vec{R}} * (u\cos\phi\ \dot{\hat{e}}_1 + u\sin\phi\ \dot{\hat{e}}_2)$$

$$= R^2\left(\dot{\hat{R}}\right)^2 + u^2\cos^2\phi\left(\dot{\hat{e}}_1\right)^2 + u^2\sin^2\phi\left(\dot{\hat{e}}_2\right)^2 + 2u\sin\phi\cos\phi\left(\dot{\hat{e}}_1\right)\left(\dot{\hat{e}}_2\right) +$$

$$2uR(\cos\phi\ \dot{\hat{R}} * \dot{\hat{e}}_1 + \sin\phi\ \dot{\hat{R}} * \dot{\hat{e}}_2)$$

$$\therefore \frac{1}{2}\mu\int_0^{r_g} du\int_0^{2\pi} d\theta\ \ u\left(\dot{\vec{x}}_{GYRO}\right)^2$$

$$= \frac{1}{2}\mu\left[R^2\left(\dot{\hat{R}}\right)^2\pi r_g^2 + \frac{\pi r_g^4}{4}\left(\dot{\hat{e}}_1\right)^2 + \frac{\pi {r_g}^4}{4}\left(\dot{\hat{e}}_2\right)^2 + 0 + 0\right]$$

***note: $\hat{e}_1, \hat{e}_2$ are turning and twisting around so they are time dependent unlike $\hat{x}, \hat{y}, \hat{z}$.

$$\mathrm{T_{GYRO}} = R^2\left(\dot{\hat{R}}\right)^2 * \tfrac{1}{2}M_{GYRO} + \tfrac{r_g^2}{8}M_{GYRO}\left(\left(\dot{\hat{e}}_1\right)^2 + \left(\dot{\hat{e}}_2\right)^2\right)$$

Recall that we need to get this as an explicit function of θ and α (and constants)

1) $\dot{\hat{R}} = ?$ "α, θ"

$\hat{R} = \sin\theta\hat{x} + cos\theta\hat{y}$

$\dot{\hat{R}} = \dot{\theta}\cos\theta\hat{x} - \dot{\theta}sin\theta\hat{y}$

$\left(\dot{\hat{R}}\right)^2 = \dot{\theta}^2(\cos^2\theta + \sin^2\theta) = \dot{\theta}^2$

2) $\left(\dot{\hat{e}}_1\right)^2 + \left(\dot{\hat{e}}_2\right)^2 = ?$ "α, θ"

This one will get messy considering we need to relate $\hat{e}_1, \hat{e}_2, \hat{e}_3$ to the lab frame. The gyro rotates in the (moving) $\hat{R}, \hat{R} \times \hat{\Omega}$ plane. Then $\hat{e}_1$ and $\hat{e}_2$ can be related to $\hat{R}$ and $\hat{\Omega}$ via the following:

$$\begin{pmatrix}\hat{e}_1\\ \hat{e}_2\end{pmatrix} = \begin{pmatrix}\cos\Omega t & \sin\Omega t\\ -\sin\Omega t & \cos\Omega t\end{pmatrix}\begin{pmatrix}\hat{R}\times\hat{\Omega}\\ \hat{R}\end{pmatrix}$$

which may be confirmed by showing that $\hat{e}_1 * \left(\hat{R} \times \hat{\Omega}\right) = \cos\Omega t$ etc. From this point $\hat{R}$ and $\hat{\Omega}$ can be expressed in terms of $\hat{x}, \hat{y}, \hat{z}$, as was done in the first iteration solution of this problem. Explicitly, for later reference:

$\hat{R} = \sin\theta\hat{x} + \cos\theta\hat{y}$

$\hat{\Omega} = -\cos\alpha\cos\theta\,\hat{x} + \cos\alpha sin\theta\,\hat{y} + sin\alpha\,\hat{z}$

Now, to solve the above system of equations using linear algebra techniques,

$$\left(\dot{\hat{e}}_1\right)^2 + \left(\dot{\hat{e}}_2\right)^2 = (\dot{\hat{e}}_1 \quad \dot{\hat{e}}_2)\begin{pmatrix}\dot{\hat{e}}_1\\ \dot{\hat{e}}_2\end{pmatrix} \equiv \dot{x}^T\dot{x}$$

Let $x = O * y$; $\quad x \equiv \begin{pmatrix}\hat{e}_1\\ \hat{e}_2\end{pmatrix}$; $\quad y \equiv \begin{pmatrix}\hat{R}\times\hat{\Omega}\\ \hat{R}\end{pmatrix}$; $\quad \begin{pmatrix}\cos\Omega t & \sin\Omega t\\ -\sin\Omega t & \cos\Omega t\end{pmatrix} = 0$

$$\dot{x}^T\dot{x} = \left[\frac{d}{dt}(O * y)\right]^T\left[\frac{d}{dt}(O * y)\right]$$

$$= \left[\dot{O}y + O\dot{y}\right]^T\left[\dot{O}y + O\dot{y}\right]$$

$$= \left[(\dot{y})^T O^T + \dot{y}^T(\dot{O})^T\right]^T\left[Oy^{\cdot} + O\dot{y}\right]$$

$$= (\dot{y})^T O^T O^{\cdot} y + y^T(\dot{O})^T O\dot{y} + (\dot{y})^T O^T O\dot{y} + y^T(\dot{O})^T\dot{O}y$$

$$= 2y^T(\dot{O})^T O\dot{y} + (\dot{y})^T\dot{y} + y^T\Omega^2 y$$

where in this last step we have used several equating properties:

$$(\dot{y})^T O^T\dot{O}y = \left((\dot{y})^T O^T\dot{O}y\right)^T = y^T(\dot{O})^T O(\dot{y})$$

This makes sense because the whole term is a scalar and the transpose of a scalar is itself. Also, we have used the fact that $O^T O = Identity\ Matrix$, since O is an orthogonal (rotation) matrix.

$$(\dot{O})^T\dot{O} = \begin{pmatrix}-\Omega\sin\Omega t & \Omega\cos\Omega t\\ -\Omega\cos\Omega t & -\Omega\sin\Omega t\end{pmatrix}^T\begin{pmatrix}-\Omega sin & \Omega cos\\ -\Omega cos & -\Omega sin\end{pmatrix} = \Omega^2\begin{pmatrix}1 & 0\\ 0 & 1\end{pmatrix}$$

$$\left(\dot{\hat{e}}_1\right)^2 + \left(\dot{\hat{e}}_2\right)^2 = 2y^T(\dot{O})^T O\dot{y} + (\dot{y})^T\dot{y} + y^T\Omega^2 y$$

$$(\dot{O})^T O = \begin{pmatrix}-\Omega\sin\Omega t & \Omega\cos\Omega t\\ -\Omega\cos\Omega t & -\Omega\sin\Omega t\end{pmatrix}^T\begin{pmatrix}cos & sin\\ -sin & cos\end{pmatrix} = -\Omega\begin{pmatrix}s & c\\ -c & s\end{pmatrix}\begin{pmatrix}c & s\\ -s & c\end{pmatrix}$$

$$= -\Omega\begin{pmatrix}0 & 1\\ -1 & 0\end{pmatrix}$$

Now, because $\left(\hat{R}\times\hat{\Omega}\right)$ and $\hat{R}$ are both unit vectors, the following is true:

$$y^T y = (\hat{R}\times\hat{\Omega}\quad\hat{R})\begin{pmatrix}\hat{R}\times\hat{\Omega}\\ \hat{R}\end{pmatrix} = \left(\hat{R}\times\hat{\Omega}\right) * \left(\hat{R}\times\hat{\Omega}\right) + \hat{R} * \hat{R} = 2$$

$$(\dot{y})^T\dot{y} = \left[\partial_t\left(\hat{R}\times\hat{\Omega}\right)\right]^2 + \left[\dot{\hat{R}}\right]^2 = \left[\partial_t\left(\hat{R}\times\hat{\Omega}\right)\right]^2 + \dot{\theta}^2$$

$$\left(\dot{\hat{e}}_1\right)^2 + \left(\dot{\hat{e}}_2\right)^2 = -2\Omega(\hat{R}\times\hat{\Omega}\quad\hat{R})\begin{pmatrix}0 & 1\\ -1 & 0\end{pmatrix}\begin{pmatrix}\partial_t\left(\hat{R}\times\hat{\Omega}\right)\\ \left(\dot{\hat{R}}\right)\end{pmatrix} + \left[\partial_t\left(\hat{R}\times\hat{\Omega}\right)\right]^2 + \dot{\theta}^2 + 2\Omega^2$$

$$= -2\Omega\left(\left(\hat{R}\times\hat{\Omega}\right)*\left(\dot{\hat{R}}\right)-\hat{R}\,\partial_{\mathrm{t}}\left(\hat{R}\times\hat{\Omega}\right)\right)+\left[\partial_{\mathrm{t}}\left(\hat{R}\times\hat{\Omega}\right)\right]^{2}+\dot{\theta}^{2}+2\Omega^{2}$$

$$= -2\Omega\left(\left(\hat{R}\times\hat{\Omega}\right)*\left(\dot{\hat{R}}\right)-\hat{R}*\left(\dot{\hat{R}}\times\hat{\Omega}+\hat{R}\times\dot{\hat{\Omega}}\right)\right)+\left[\partial_{\mathrm{t}}\left(\hat{R}\times\hat{\Omega}\right)\right]^{2}+\dot{\theta}^{2}+2\Omega^{2}$$

Using the vector identities $A\times B=-B\times A$ and $A*(B\times C)=(A\times B)*C$ to rearrange the second term within the larger term that is multiplied by -2Ω we get:

$$= -4\Omega\left(\hat{R}\times\hat{\Omega}\right)*\dot{\hat{R}}+\left[\partial_{\mathrm{t}}\left(\hat{R}\times\hat{\Omega}\right)\right]^{2}+\dot{\theta}^{2}+2\Omega^{2}$$

To get $\hat{R}\ and\ \hat{\Omega}$ in terms of $\theta\ and\ \alpha$,

$$\hat{R}\times\hat{\Omega}=(\sin\theta\,\hat{x}+\cos\theta\,\hat{y})\times(-\cos\alpha\cos\theta\,\hat{x}+\cos\alpha\sin\theta\,\hat{y}+\sin\alpha\,\hat{z})$$

$$=\sin\theta(\cos\alpha\sin\theta\,\hat{z}+\sin\alpha(-\hat{y}))+\cos\theta(\cos\alpha\cos\theta\,\hat{z}+\sin\alpha\,\hat{x})$$

$$=\sin\alpha\cos\theta\,\hat{x}-\sin\alpha\sin\theta\,\hat{y}+\cos\alpha\,\hat{z}$$

$$\therefore\left(\hat{R}\times\hat{\Omega}\right)*\dot{\hat{R}}=(\sin\alpha\cos\theta\,\hat{x}-\sin\alpha\sin\theta\,\hat{y}+\cos\alpha\,\hat{z})*(\cos\theta\,\hat{x}-\sin\theta\,\hat{y})\dot{\theta}$$

$$\left(\hat{R}\times\hat{\Omega}\right)*\dot{\hat{R}}=\dot{\theta}(\sin\alpha\cos^{2}\theta+\sin\alpha\sin^{2}\theta)$$

$$=\dot{\theta}\sin\alpha$$

$$\partial_{\mathrm{t}}\left(\hat{R}\times\hat{\Omega}\right)=(\dot{\alpha}\cos\alpha\cos\theta$$

$$-\dot{\theta}\sin\alpha\sin\theta)\hat{x}-(\dot{\alpha}\cos\alpha\sin\theta+\dot{\theta}\sin\alpha\cos\theta)\hat{y}-(\dot{\alpha}\sin\alpha)\hat{z}$$

$$\left[\partial_{\mathrm{t}}\left(\hat{R}\times\hat{\Omega}\right)\right]^{2}=\dot{\alpha}^{2}\cos^{2}\alpha+\dot{\theta}^{2}\sin^{2}\alpha+\dot{\alpha}^{2}\sin^{2}\alpha$$

$$=\dot{\alpha}^{2}+\dot{\theta}^{2}\sin^{2}\alpha$$

$$\left(\dot{\hat{e}}_{1}\right)^{2}+\left(\dot{\hat{e}}_{2}\right)^{2}=-4\Omega\dot{\theta}\sin\alpha+\dot{\alpha}^{2}+\dot{\theta}^{2}\sin^{2}\alpha+\dot{\theta}^{2}+2\Omega^{2}$$

$$\therefore\quad \mathbf{T_{GYRO}}=\frac{\mathbf{1}}{\mathbf{2}}\boldsymbol{M_{GYRO}R^{2}\dot{\theta}^{2}}+\frac{\boldsymbol{r_{g}^{2}}}{\mathbf{8}}\boldsymbol{M_{GYRO}}(-\mathbf{4\Omega\dot{\theta}\sin\alpha}+\boldsymbol{\dot{\alpha}^{2}}+\boldsymbol{\dot{\theta}^{2}}\mathbf{\sin^{2}\alpha}+\boldsymbol{\dot{\theta}^{2}}+\mathbf{2\Omega^{2}})$$

$$\therefore \quad \boldsymbol{L(\theta,\alpha) = \frac{1}{2}\left(I_{BIKE}M_{GYRO}R^2 + \frac{1}{4}M_{GYRO}r_g^2(1+\sin^2\alpha)\right)\dot{\theta}^2 + \frac{1}{8}M_{GYRO}r_g^2\dot{\alpha}^2}$$

$$\boldsymbol{-\frac{1}{2}M_{GYRO}r_g^2\Omega\dot{\theta}\sin\alpha + \frac{1}{4}M_{GYRO}r_g^2\Omega^2 - V_o\cos\theta}$$

$$\frac{\partial L}{d\theta} = \frac{d}{dt}\left(\frac{\partial L}{\partial\dot{\theta}}\right)$$

$$V_o\sin\theta =$$

$$\frac{d}{dt}\left[\left(I_{BIKE} + M_{GYRO}R^2 + \frac{1}{4}M_{GYRO}r_g^2(1+\sin^2\alpha)\right)\dot{\theta} - \frac{1}{2}M_{GYRO}r_g^2\Omega\sin\alpha\right]$$

$$\therefore \quad \boldsymbol{0 = \left(I_{BIKE} + M_{GYRO}R^2 + \frac{1}{4}M_{GYRO}r_g^2(1+\sin^2\alpha)\right)\ddot{\theta} + \frac{1}{2}M_{GYRO}r_g^2\dot{\alpha}\dot{\theta}\sin\alpha\cos\alpha} \ldots$$

$$\ldots \boldsymbol{-\frac{1}{2}M_{GYRO}r_g^2\Omega\frac{d(\sin\alpha)}{dt} - V_o\sin\theta}$$

$$\frac{\partial L}{\partial\alpha} = \frac{d}{dt}\left(\frac{\partial L}{\partial\dot{\alpha}}\right)$$

$$\frac{1}{2} * \frac{1}{4}M_{GYRO}r_g^2 * 2\dot{\theta}^2\sin\alpha\cos\alpha - \frac{1}{2}M_{GYRO}r_g^2\Omega\dot{\theta}\cos\alpha = \frac{d}{dt}\left[\frac{1}{4}M_{GYRO}r_g^2\dot{\alpha}\right]$$

$$M_{GYRO}r_g^2\,\dot{\theta}^2\sin\alpha\cos\alpha - 2M_{GYRO}r_g^2\Omega\,\dot{\theta}\cos\alpha - M_{GYRO}r_g^2\ddot{\alpha} = 0$$

$$\therefore \quad \boldsymbol{0 = \ddot{\alpha} - \sin\alpha\cos\alpha\,\dot{\theta} + 2\Omega\dot{\theta}\cos\alpha}$$